Glued-in rods for timber structures - An experimental study of softening behaviour

Serrano, Erik

Published in:
Materials and Structures

DOI:
10.1007/BF02480593

2001

Document Version:
Early version, also known as pre-print

Glued-in Rods for Timber Structures – An Experimental Study of Softening Behaviour

Erik Serrano

Division of Structural Mechanics, Lund University

P.O. Box 118, SE-221 00, Lund, Sweden

Submitted for publication in Materials and Structures

Abstract

A test method to obtain the strength and the fracture characteristics of the bond of glued-in rods for timber structures is presented. Test results from a series of tests using the proposed method are also given. The test method makes it possible to record the complete stress-displacement response of small test specimens. This response includes the softening behaviour after peak stress, i.e. the decreasing stress at increasing deformation. The test series include three adhesives, two rod materials, four load-to-grain angles and two timber qualities with different densities. A method to evaluate the fracture-softening behaviour is also proposed. The fracture softening is evaluated by using only a part of the stress-displacement curve. The part used in the evaluation is determined in terms of the slope of the descending part of the stress-displacement curve.

1 Introduction

1.1 Background

Glued-in rods are used in timber engineering to join beams and columns. The rods used are often threaded steel rods or ribbed reinforcement bars. The glued-in rod connection results in stiff and strong joints, which can be used, e.g. for frame corners and column foundations. Glued-in rods have also been used to reinforce timber elements in areas of high stresses perpendicular to the grain such as in curved or tapered beams or at notches. Although

glued-in rods have been used for several years, there is no current normative standard in the European timber code, EC5. The present paper presents a part of an ongoing European research programme, "Glued-in Rods for Timber Structures – GIROD", aiming at developing such code proposals. The paper describes a test method to obtain the strength and the fracture characteristics of the bond of glued-in rods. Test results from using the proposed method are also presented. The fracture characteristics are recorded as the complete stress-displacement response of small test specimens. This response includes the softening behaviour after peak stress, i.e. the decreasing stress at increasing deformation.

1.2 Previous Work

Previous experimental work on glued-in rods for timber has mainly concerned the testing of structural-sized specimens and the results have been used to obtain empirical design equations. Examples of such experimental programmes are Riberholt [1], Ehlbeck [2], Kangas [3], Deng [4] and Aicher et al. [5]. Although testing on structural-sized specimens is necessary for the verification and calibration of theoretical models, such testing is usually not practicable for obtaining material-property parameters, e.g. parameters that define the local strength and fracture properties of the bond.

Tests on wood and wood-adhesive bonds to obtain fracture characteristics in terms of the fracture-softening behaviour have been performed.e.g. by Boström [6] and Wernersson [7]. Boström reports on a test method for small, notched, wood specimens in tension (mode I) and in shear (mode II), to obtain their complete stress-displacement response, including the descending, strain-softening part. Using a similar technique, Wernersson performed tests on wood-adhesive bonds in mode I, II and in mixed modes.

In a preliminary study on glued-in rods by Johansson et al. [8], a test series on small glued-in rod specimens was presented. The method used in the present study is a further development and simplification of this, partly based on the experiences gained in that preliminary study.

1.3 Present Study

Aim

The present study concerns an experimental method to obtain the fracture characteristics of glued-in rods for timber structures. These characteristics involve the local strength of the adhesive bond, its fracture energy or critical energy release rate, and its strain-softening behaviour. The main aim is to

record the local shear-stress versus shear-slip relation, and from this evaluate parameters for the strength, fracture energy and fracture softening. These material data are needed as input for theoretical material models used in numerical finite element simulations. Such numerical simulations can be used to calibrate rational hand-calculation models, which in turn can constitute the basis of future design equations.

Experimental Programme

The experimental programme involves testing of rods glued with three different adhesives: a fibre-reinforced phenol-resorcinol (PRF), a 2-component polyurethane (PUR) and an epoxy (EPX). These tests are performed with threaded steel rods (M16), glued parallel to the grain in pieces of wood cut from glulam beams of two different qualities. The EPX is also tested for various load-to-grain angles for one of the timber qualities and, finally, a series of tests is performed on a glass-fibre reinforced polyester (FRP) rod, again using the EPX. For each kind of specimen five nominally equal samples were tested.

2 Materials and Methods

2.1 General Remarks

In testing for mechanical properties, e.g. of an adhesive bond line, two markedly different approaches in sample preparation can be used: a) cut out a small, representative test specimen of appropriate size and shape from the structure to be analysed, or b) prepare a small test specimen of the size required in the test.

These two approaches have their respective advantages and disadvantages. The first approach is appealing because a test specimen is cut from a structure manufactured in the same way as it would be in practice. For the present application this approach would mean that a structural-sized rod is glued into a timber beam which is then cut (sliced) into pieces of appropriate size. If this approach is used, the curing of the adhesive will take place under circumstances similar to those used in practice. The test specimen is thus a representative sample of a structural-sized glued-in rod. The major drawback of this method is that the cutting of the rod might damage the specimen. Another drawback, is that the sample preparation, i.e. the cutting of the specimens, can be somewhat difficult to perform since it requires special sawing facilities.

The second approach is a more standard approach, at least for pure mechanical testing of materials. In the present context this approach means that a rod of short length is glued into a small piece of wood. Producing a specimen using this approach, the question arises whether the gluing and curing conditions of the adhesive are the same as for structural-sized rods. It is difficult, using a short glued-in length, to ensure a high pressure in the bondline during curing. This means that boundary effects during curing might have an impact on the strength of the bondline. One example of such boundary effects, related to the use of PUR-adhesive, is the forming of CO_2-bubbles, which can become intense at free surfaces of the adhesive (foaming).

2.2 Materials and Climate Conditions

Three adhesives and two rod materials, as described above, were tested. All samples were prepared using pieces of wood cut from spruce glulam beams of two different strength classes, C35 and C24. The glulam beams were stored for several months in standard climate, 20°C, 65%RH, before sample preparation. The gluing and curing as well as the storing of the finished specimens also took place in this climate. All specimens were cured for at least seven days prior to testing.

The density and the moisture content of the wood were determined by cutting out small pieces close to the bondline and then weighing the pieces in air and under water. The specimens were subsequently dried at 105°C for 24 hours and again weighed. The density values reported are calculated as (dry mass)/(volume at 20°C, 65%RH)

2.3 Sample Preparation

Both the above methods of producing test specimens were investigated in a series of pre-tests, not reported here. The conclusion was that the second method, i.e. the gluing of small specimens, was the most reliable one, and therefore, this method was used in the main test series, reported here.

Glulam beams with a 120 mm square cross section were split into four pieces of 48×48 mm^2. Each such piece was then cut to a thickness of 40 mm. In each piece, a hole of a diameter ϕ=17 mm, was drilled through the entire piece. From a threaded steel rod (M16), strength class 8.8, 90 mm long pieces were cut and further machined in a lathe, leaving a threaded length of 8 mm. Fig. 1 shows how the wood pieces were cut from the beams.

After drilling, the holes were partially filled from one end with Tack-It, which is a kind of synthetic clay used to fix posters etc. An 8.5 mm deep

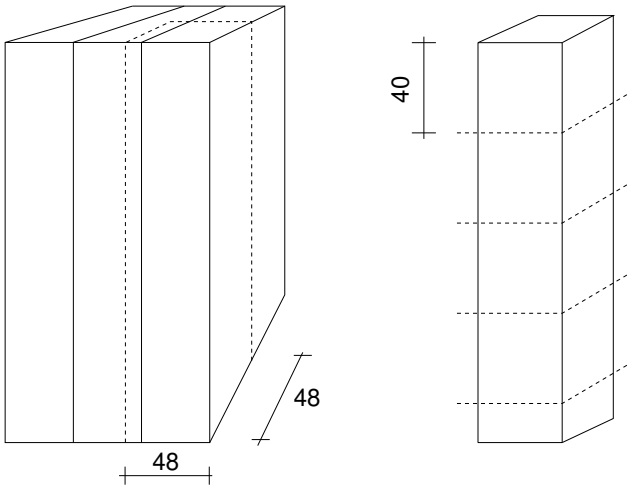

Figure 1: The specimens were cut from glulam beams.

hole was left, at the bottom of which a circular, 0.5 mm thick, Teflon film was put, leaving an 8 mm deep hole for the threaded rod to be glued into.

Adhesive was poured into the holes and the rods placed in the holes. To ensure a good filling out of the grooves of the threads, glue was also spread on the thread of the bolts. A fixing device was used to ensure that the bolts were glued in and fixed in the desired direction during curing. In order to ensure a centrally placed bolt in the drilled hole, three metal clips were pressed into the synthetic clay so that the bolt was securely fixed at the centre of the hole. After curing of the adhesive the synthetic clay and the Teflon film were removed.

The same principle for sample preparation was used for the tests performed on the FRP rod. The 16 mm diameter rods were cut into 90 mm long pieces and were then machined to 12 mm diameter except for the 8 mm at one end. The FRP rods have a smooth surface and to improve the adhesion of the glue, they were lightly sanded by hand and then wiped clean using a cloth soaked with alcohol.

Three additional load-to-grain angles were tested: 22.5°, 45° and 90° respectively. Each specimen was cut out so that the bond would consist of wood from only one lamination. This means that the 90° specimens, for instance, were cut almost in the radial direction of the wood, cf. Fig. 2.

2.4 Test Set-ups and Testing Conditions

All tests were performed using displacement control to make possible a recording of the softening behaviour of the bondline. Several pre-tests were

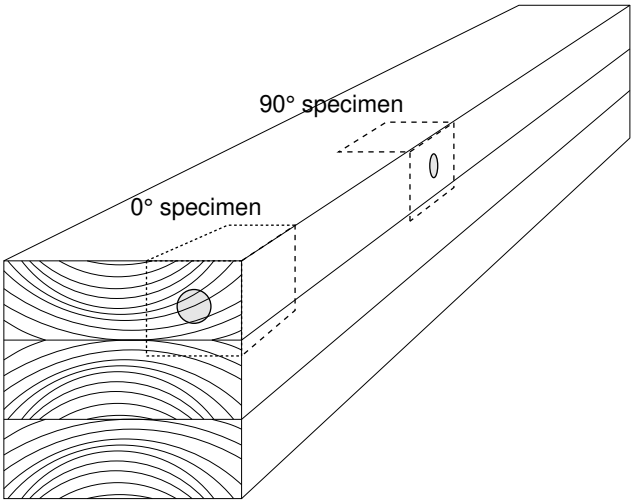

Figure 2: Specimen cutout for two load-to-grain angles.

performed to find a suitable rate of displacement, so that the peak load could be obtained within a few minutes and the total time to failure would be about 10–15 minutes.

The test specimens were placed on a self-aligning plate, which in turn was mounted into the lower hydraulic grips of the testing machine. The self-aligning plate was used in order to achieve a more uniform stress distribution at the contact surface. The specimen and the set-up is shown in Fig. 3.

The initial speed of the hydraulic actuator was 0.003 mm/s (cross-head speed). After a 40% load drop after peak load, the speed was gradually increased, and the final speed was 0.03 mm/s. In addition to the original plan, including five nominally equal tests for each material combination, a decision was made to investigate the characteristics at unloading after peak stress for one specimen. Here, unloading means decreasing deformation. The unloading sequence of these tests was automatically initiated by the software of the test system. The unloading was set to take place after a 20% load drop. After the unloading down to zero load, a new loading sequence was run until complete failure of the specimen was achieved.

2.5 Methods of Evaluation

Strength and Work to Failure

From the tests it is straightforward to evaluate the strength of the bond (load divided by fracture area), and to integrate the stress-displacement curve to obtain the work to failure. Here, failure is defined either as a total separation

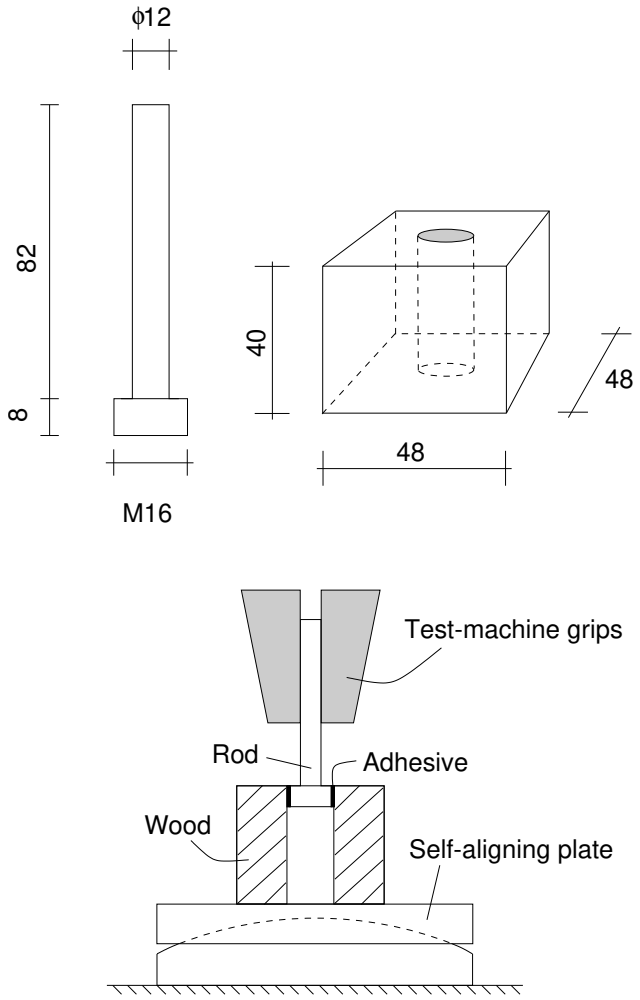

Figure 3: Test specimen and set-up.

of the bondline with zero load-bearing capacity, or, if the bondline at the end of the test still has a load-bearing capacity due to friction, at a 10 mm deformation of the rod.

When integrating the stress-deformation curve, it was assumed that the fracture area was equal to the area of a cylinder of 16 mm diameter. The lengths of the fracture surfaces were measured after splitting the test specimens to obtain specimens for the density measurements.

The bond shear strength obtained in this way is estimated to be representative, since the short length and the support conditions of the specimen contribute to a uniform stress distribution and small peel stresses. The evaluation of the fracture energy of the bond requires some further consideration since the recorded work to failure is mainly due to friction after the local fracture has taken place in the bond layer. As an example, consider the PRF-bonded specimens, which failed at the thread-adhesive interface. Bearing in mind that the pitch of the used thread is 2 mm, it is obvious that the PRF bondline has fractured completely after a deformation of about 0.5–1.0 mm. The remaining load-bearing capacity is therefore completely due to friction. To overcome such difficulties in the test evaluation a trial and error approach using nonlinear finite element simulations of the tests can be used, fitting local bond strength (shear and peel strength) and fracture energies until the test results (strength, energy and shape of curve) can be reproduced numerically. Another alternative to overcome the difficulty in fracture energy evaluation is discussed and applied below.

Evaluation of Shear-slip Curve

To estimate the initial stiffness, all slopes from zero to maximum load were calculated using least square fits, for intervals of length of 25% of the maximum load. Thesteepest slope was chosen as initial stiffness. Fig. 4 shows the results of the evaluation process for one of the PRF specimens. Three curves are shown. One represents the recorded test data with the load divided by the nominal shear area. As is evident, the slope of the curve increases initially, probably due to rough contact surfaces and the initial movement of the self-aligning plate of the test set-up. Following this initial nonlinear region, an almost perfectly linear part is found, followed by nonlinearities close to peak stress, probably due to an initiating fracture and possibly to plasticity. The second curve shown in Fig. 4 represents the response with the approximated initial elastic stiffness. Finally a curve with the elastic deformations subtracted is shown. For this curve the deformation represents the additional deformation due to damage in the bondline.

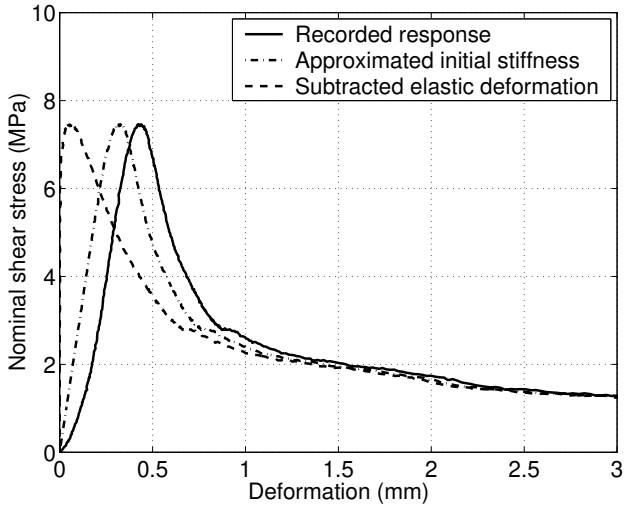

Figure 4: Evaluation of the initial stiffness.

Characterisation of Fracture Softening

The total energy "consumed" during the tests is mostly due to friction, after the fracture has taken place, and is not a parameter of large influence on the load-bearing capacity in a structural-sized specimen. Therefore, instead of using the area below the complete stress-displacement curve as a measure of the fracture energy of the bond, the slope of the descending branch is used. This slope is the critical one for a stable response and, furthermore, for structural-sized bonds, the total deformation before collapse is in the range of 1–2 mm rather than of 8–10 mm, which was the typical deformation at complete failure for most of the small specimens tested. For bonds that show negligible plastic response before peak stress, a typical slope of the descending part, together with the strength, define a triangular area that can be used as a measure of the fracture energy. For the cases of considerable plastic response before peak stress, the slope together with the strength and the stress-displacement curve prior to peak stress, define another effective area. This is shown schematically in Fig. 5 for the case with plastic response before peak stress. Note that the initial elastic response of this curve has been subtracted, so that the deformation corresponds to the plastic strain before peak stress and, to the relative slip due to damage or microcracking in the bondline after peak stress.

After subtracting the elastic deformations from the recorded shear-slip response, the slope of the descending part of the shear-slip curve was evaluated with the same algorithm as described above for the evaluation of the initial

elastic stiffness. This means that here, the fracture-softening properties are characterised by the steepest 25% of the maximum load interval.

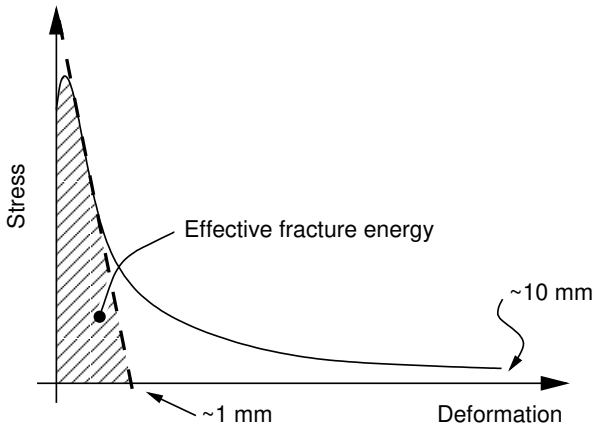

Figure 5: An example of how to evaluate the fracture softening of the specimen.

3 Results and Discussion

3.1 General Remarks

A total of 62 tests were performed, 61 of which are included in the results. The test rejected was one of the FRP specimens, which failed in the rod itself, probably due to damage caused to the rod in the manufacturing of the specimen. The different material combinations and load-to-grain angles, together with the result statistics, are summarised in Table 1.

The table gives the average and coefficient of variation (COV) of density, moisture content, strength, negative slope after peak stress, and work to failure respectively. For each nominally equal material combination, five replications were performed with monotonically increasing deformation of the testing machine's crosshead. In addition, for each material combination, one test was performed with unloading of the specimen in the softening region, after peak stress. The strength and initial elastic slope statistics are all based on six replications, while the other statistics are based on five replications since the unloading part of the curve complicates the evaluation of these quantities. The statistics from the FRP-rod tests are based on seven and six tests respectively. It was possible to record the complete stress-slip curve for

Table 1: Results from tests, mean values (COV in %).

Material combination (-)	Density (kg/m^3)		MC (%)		Strength (MPa)		Negative Stiffness (MPa/mm)		Work to failure (kJ/m^2)	
St./C35/PRF/0°	449	(2)	14.4	(1)	7.05	(6)	8.6	(20)	12	(20)
St./C35/PUR/0°	492	(2)	13.2	(2)	10.5	(10)	62	(23)	9.6	(9)
St./C35/EPX/0°	462	(1)	12.8	(1)	13.1	(10)	60	(18)	22	(14)
St./C24/PRF/0°	348	(4)	12.8	(2)	6.18	(5)	7.0	(20)	14	(14)
St./C24/PUR/0°	368	(3)	13.1	(2)	10.6	(5)	62	(4)	8.0	(9)
St./C24/EPX/0°	341	(3)	12.7	(3)	11.0	(12)	52	(8)	21	(18)
St./C35/EPX/22.5°	454	(1)	13.8	(1)	12.8	(4)	48	(13)	23	(4)
St./C35/EPX/45°	429	(10)	13.3	(2)	10.7	(6)	28	(19)	25	(10)
St./C35/EPX/90°	469	(6)	13.5	(2)	7.12	(6)	3.1	(42)	25	(4)
FRP/C35/EPX/0°	451	(1)	13.5	(3)	11.8	(7)	44	(7)	28	(10)

all the material combinations and examples of such curves are given below, together with the discussions about the influence of the adhesive type and of the load-to-grain angle.

3.2 Failure Modes

The failure modes obtained in the tests are of three types, each typical for one type of adhesive:

1. Failure in the adhesive at the threading of the bolt. This failure mode was obtained only for the PRF adhesive covering about 75-100% of the fracture area. The remaining fracture area presented a wood-interface failure.

2. Failure in the adhesive close to the wood. This failure was obtained only for the PUR specimens and, covered 100% of the fracture area.

3. Failure in the wood in the vicinity of the adhesive. Note that this wood failure is not characterised by a large plug being pushed out, but rather by a wood-interface failure due to a weak boundary layer. This failure type was obtained only for the EPX specimens. For the 0° load-to-grain angle tests, there was a fairly large amount of wood fibres visible on the adhesive after failure. For the other load-to-grain angles the fracture surface was almost free from fibres.

In Fig. 6, three examples of the different failure modes obtained are shown. The reason for these distinctively different failure modes can be explained as follows: The adhesion of the PRF to the steel is negligible, and in combination with the PRF's tendency to shrink during curing, an initial lack of fit between the adhesive and the threads of the bolt was observed. This results in stress concentrations at the thread/adhesive interface and also a low initial stiffness of the joint. The large stress concentrations lead to the failure at the bolt/adhesive interface region. The PRF adhesive thus works as way to cast threads in the drilled hole and the joint performs more like a bolted connection than an adhesive bond. From the stress-displacement curves, cf. Fig. 4, it is also appearent that there is a considerable amount of frictional work performed during the test. The pitch of the threads used (M16) is 2 mm, and, since the failure takes place at the tip of the threads, an approximately 1 mm deformation implies that the bond line has come to a complete failure.

The curing of the PUR adhesive relies on the possibility of taking up moisture from the adherends and the surrounding air. The chemical reaction

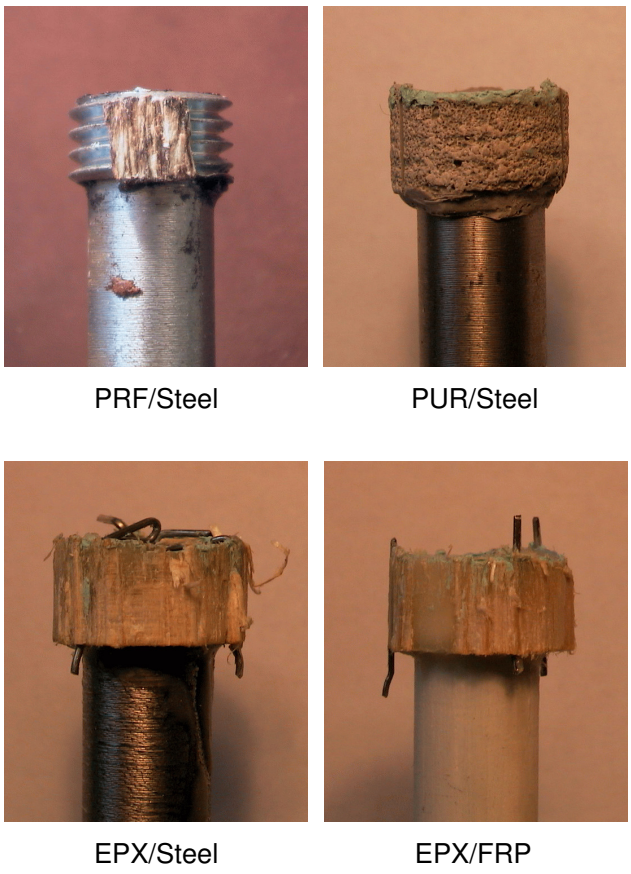

Figure 6: Failure surfaces for PRF, PUR and EPX adhesives respectively.

forms CO_2, which causes bubbles to form in the bondline. In the case of low or no pressure at all during curing, this bubble formation becomes intense. The failure surfaces of the PUR specimens had bubbles of sizes in the order of 0.1–0.5 mm. The bubble formation can be expected to be more intense at the free surface of the adhesive and at the wood interface where more moisture is available. This explains why the fracture surface is located close to the the wood/adhesive interface.

The EPX adhesive gives strong bondlines with good adhesion to the steel, the wood and the FRP rods. The failure is therefore located in the wood, which in this case is the weakest link.

3.3 Influence of Adhesive Type and Rod Material

Based on the above discussion of the failure modes, the strength of the adhesives should form a sequence showing increasing strength in the order of: PRF, PUR and EPX. The mean strength as reported above also confirms this. In Fig. 7, hand-drawn mean curves, one for each adhesive, show the influence on the stress-displacement response of the adhesive type. A mean curve for the tests performed on the FRP rod is also shown. The curves show the response with the elastic deformation subtracted. It is clear from the curves that the PUR and the EPX are similar with respect to the slope of the descending part of the curve, while the PRF adhesive shows a much more ductile behaviour.

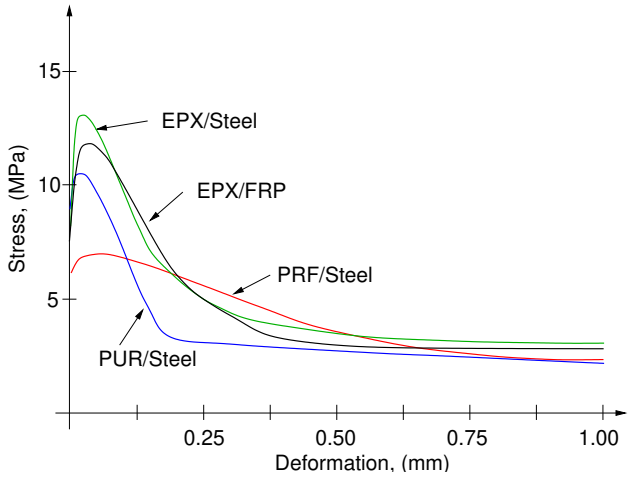

Figure 7: Influence of adhesive type and rod material on stress-displacement response. Timber C35, 0° load-to-grain angle.

3.4 Influence of Wood Density

The influence of the wood density on the strength is complicated to assess since the density of the wood can be expected to have an influence in at least three ways. Firstly, it is often assumed that the density and the strength of the wood are positively correlated; secondly, a change in density could mean a change in adhesion to the wood, and, finally a change of density can result in different modulus of elasticity, which in turn can affect the strength of a glued-in rod due to a change of the stress-distribution. There is a statistically significant difference (0.05 level) in density between the two timber qualities, but this difference only results in a significant difference (0.05 level) in strength for the PRF and EPX adhesives.

3.5 Influence of Load-to-grain Angle

The influence of the load-to-grain angle on the performance of the bond is of several different types. Changing the load-to-grain angle will affect the effective moduli of elasticity of the adherend. It is also probable that the adhesion of the glue to the wood is different for different orientations, since the surface roughness of the drilled hole depends on the orientation of the grain. Finally it should be emphasised that a load-to-grain angle other than 0° will always result in parts of the wood being stressed in longitudinal shear (τ_{rl}) and other parts in rolling shear (τ_{rt}). Therefore, the results from such a test will be some kind of average, taken in the circumferential direction, which includes both shearing modes. If the strengths in the two directions differ considerably, the fracture will be a propagating one (in the circumferential direction). Such a propagating failure will lead to an apparently ductile behaviour on a larger scale, i.e. the scale on which the present tests are monitored. Fig. 8 shows the influence on the stress-displacement response, with the elastic deformations subtracted. The behaviour of the tests are increasingly ductile as the load-to-grain angle changes from 0° to 90°.

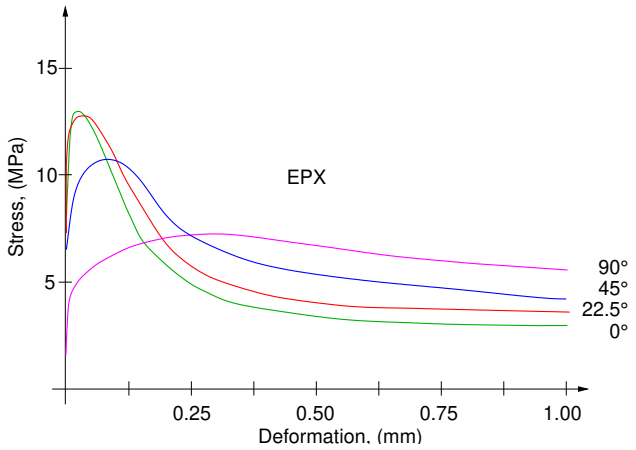

Figure 8: Influence of load-to-grain angle on stress-displacement response. Epoxy adhesive, timber C35, steel rod.

4 Conclusions

The following conclusions can be drawn from the present work:

- Test methods:
  - Testing for fracture-softening properties is demanding, and several pre-tests to determine a proper test set-up was needed.
  - A test set-up was developed, which proved to work well from a practical point of view and was estimated to give representative and reproducible results.
- Test results:
  - It is possible to obtain the complete shear-stress versus shear-slip response of small glued-in rod specimens.
  - Characteristic and significantly different results were obtained for different adhesives in terms of stress-slip performance, strength, fracture softening and fracture mechanism.
- Methods of test-result evaluation:
  - A method of evaluating the test results in terms of strength and fracture-softening properties has been proposed. The fracture softening is evaluated using only a part of the stress-displacement curve obtained from tests. This part is defined in terms of the slope of the descending part of the stress-displacement response.

5 Acknowledgements

The GIROD project involves the following research institutes: SP – the Swedish National Testing and Research Institute, FMPA Otto-Graf Institute (Germany), the University of Karlsruhe (Germany), TRADA Technology (UK) and Lund University (Sweden). The financial support through grant no. SMT4-CT97-2199 by the European Commission (DG XII) and the co-operation of the partners involved in this research project are gratefully acknowledged.

This research was also in part financially supported by the Swedish Council for Building Research (BFR), project no. 19960633. This support is also gratefully acknowledged.

Finally, a special thanks is directed to Mrs. Rizalina Brillante, for her skilful running of the testing machine.

References

[1] Riberholt, H. 'Glued bolts in glulam'. Report R210. (Department of Structural Engineering, Technical University of Denmark, Lyngby, Denmark, 1986).

[2] Ehlbeck, J. and Siebert, W. 'Praktikable Einleimmethoden und Wirkungsweisen von eingeleimten Gewindstangen unter Axialbelastung bei Übertragung von grossen Kräften und bei Aufnahme von Querzugkräften in Biegeträgern'. Report. (University of Karlsruhe, Germany,1987).

[3] Kangas, J. 'Joints of glulam structures based on glued-in ribbed steel rods.' VTT Publications 196. (Technical research centre of Finland, Espoo, Finland, 1994).

[4] Deng, J. X. 'Strength of epoxy bonded steel connections in glue laminated timber'. PhD-thesis. Civil engineering research report 97/4. (Dept. of Civil Engineering, University of Canterbury, Christchurch, New Zealand, 1997).

[5] Aicher, S., Gustafsson, P. J. and Wolf, M. 'Load displacement and bond strength of glued-in rods in timber influenced by adhesive, wood density, rod slenderness and diameter'. Proceedings 1st RILEM Symposium on timber engineering, Stockholm, 1999. Ed. L. Boström. (RILEM Publications S.A.R.L. Cachan, France, 1999) pp. 369–378.

[6] Boström, L. 'Method for determination of the softening behaviour of wood and the applicability of a nonlinear fracture mechanics model'. PhD thesis. Report TVBM-1012. (Lund University, Division of Building Materials, Lund, Sweden, 1992).

[7] Wernersson, H. 'Fracture characterization of wood adhesive joints'. PhD thesis. Report TVSM-1006. (Lund University, Division of Structural Mechanics, Lund, Sweden, 1994).

[8] Johansson, C-J., Serrano, E., Gustafsson, P. J. and Enquist, B. 'Axial strength of glued-in bolts. Calculation model based on non-linear fracture mechanics - A preliminary study'. Proceedings CIB-W18. Meeting twenty-eight. Copenhagen, Denmark 1995. (University of Karlsruhe, Germany, 1995).